Generalization of Interfacial Electrohydrodynamics in the Presence of Hydrophobic Interactions in Narrow Fluidic Confinements

Suman Chakraborty*

Department of Mechanical Engineering, Indian Institute of Technology, Kharagpur-721302, India

(Received 3 December 2007; published 7 March 2008)

We show that the interfacial electromechanics in narrow fluidic confinements exhibits a universal dependence with the intrinsic surface-wettability characteristics, independent of the details of the bulk flow actuating mechanisms. Towards this proposition, we develop a generalized mesoscale model, which is extensively tested for combined electro-osmotic and pressure-driven nanochannel flows. Agreement with the molecular dynamics simulations is found to be quantitative.

DOI: 10.1103/PhysRevLett.100.097801 PACS numbers: 68.15.+e, 47.45.Gx, 82.45.−h

Electrohydrodynamics within the electrical double layer (EDL) is central to the understanding of the transport characteristics of charged colloidal systems [1] in micro- or nanoscale fluidic devices and systems. The concerned applications are truly diverse in nature, encompassing the manipulation of biological macromolecules and cells in lab-on-a-chip based high throughput systems. Significant electrokinetic effects (such as electro-osmosis, electrophoresis, streaming potential) governing the physical behavior of these systems may have far-ranging scientific and technological consequences, since these can provide stringently controllable, rapid, and efficient means for manipulating flows in narrow fluidic confinements. Traditionally (and perhaps nonphysically), these effects have been postulated to be somewhat uncorrelated with the other fundamental and intrinsic transport characteristics of narrow confinements, such as the interfacial wettability conditions, particularly over the experimentally tractable spatiotemporal regimes. This deficit in fundamental understanding has evidently stemmed from the complexities in describing the underlying thermofluidic interactions at physical scales that are substantially larger than those addressed in the detailed molecular scale models.

In nanochannel flows, hydrophobic interactions are likely to trigger an apparent slip phenomenon, due to a spontaneous transition of the liquid to a less dense phase in the interfacial region [2]. This, in turn, is expected to alter the so-called zeta potential (ζ), which is classically defined as the electrical potential in the plane of ''zero slip,'' in a dynamically evolving manner. Despite the recent advancements in the analysis of electrohydrodynamics in small scale systems, several fundamental aspects of this interaction still remain to be poorly understood, especially within the limits of experimentally resolvable physical scales.

Here what is proposed is believed to be the first generalized mesoscale description depicting a coupling between the complex hydrophobic interactions and the electromechanics within the EDL in narrow fluidic confinements. On the basis of the resultant conjecture, we arrive at a universal expression of an augmented slip parameter, as a combined function of an equivalent interfacial potential and an apparent slip length, independent of the details of the flow actuation mechanism, by appealing to a generalized definition of the effective zeta potential. Without sacrificing the requirements of a consistent representation, the present modeling effort further reduces the necessity of executing explicit and expensive molecular dynamics (MD) simulations for capturing the underlying physics.

Two new features are introduced into the present model for achieving the above-mentioned feat, in an effort to discover a universal interplay between the EDL electrohydrodynamics and the hydrophobic interactions in micro- or nanochannels. First, the hydrophobicity at the substrate-fluid interface is explicitly represented through an order-parameter description. This is achieved by exploiting a direct relationship between the effective contact angle and the surface value of the order parameter. The model is further sensitized to the rapidly varying small length scale fluctuations of the order parameter about its slowly-varying components, as well as the modifications of the local molecular fields due to the replacement of polar liquids by rigid walls (triggering the possibility of separation-induced phase transition processes). Second, the structuration-induced oscillations in the micro-ion density profiles are accounted for through an electrical potential correction in the classical electromechanical description. The coupling between the electrohydrodynamic and hydrophobic interactions is achieved by postulating this correction term as an explicit function of the hydrodynamic order-parameter distribution (mimicking the variations in the fluid phase density profile). With the above physical considerations, it is established that the physics of coupling between hydrophobic interactions in narrow fluidic confinements and the electromechanics within the EDL can be quantitatively reproduced by the generalized order-parameter model, without explicitly resolving the molecular details.

The present model stems its physical description from the free energy (F) of the system, which comprises two major components ($F = F_1 + F_2$). The first component, F_1, is the so-called Ginzburg-Landau free energy for a binary mixture. Physical origin of the existence of such a

binary mixture despite intending a single-phase (liquid) bulk fluidic transport may be attributed to a local phase transition at the substrate-fluid interface, triggering the generic and spontaneous formation of a gas layer in the vicinity [2]. In the present free-energy description, the above effects are implicitly captured by introducing a phase-field order parameter (effectively, a relative phase concentration distribution), $\phi = (n_1 - n_2)/(n_1 + n_2)$, where n_i are the number densities of the two species. The concerned free-energy functional is described elsewhere [3,4] and is not repeated here for the sake of brevity. The chemical potential corresponding to F_1, i.e., $\mu(\phi) = \frac{\delta F_1}{\delta \phi}$, is further corrected by accounting for an excess equivalent chemical potential due to excluded volume effects (since hydrophobic units are not thermodynamically favored to form hydrogen bonds with water molecules) and separation-induced phase transition (since the loss of hydrogen bonds near the hydrophobic surfaces effectively expels liquid water, energetically favoring the inception of thin vapor layers) [3].

The second component of the free energy, F_2, is electrochemical in nature and comprises the usual Poisson-Boltzmann (PB) free energy with pertinent correction terms. These correction terms are necessary because of the fact that in the PB theory, the ions are treated as independent charged particles interacting with an external electrostatic potential as a mean-field approximation, without taking into account the correlations between ion positions. Further, the PB theory treats ions as pointlike objects that are solely subjected to electrostatic interactions in a dielectric medium. In reality, however, extended forms of these interactions, such as non-Coulombic interactions between ion pairs, may turn out to be significant. These interactions, particularly significant for narrow confinements, include short-range steric repulsions, interactions with the polar solvent molecules, and short-range interactions with the confining charged surfaces. Evidently, the replacement of the solvent by a continuous medium cannot be precise when the interionic distance is comparable to the solvent molecular size. Thus, in cases of high ionic densities, the discreteness of the solvent is expected to bear a significant consequence on the potential distribution. Therefore, in addition to the electrostatic free energy and entropic contributions to the free energy of ions, hydration interactions between the ionic constituents also feature in the present description of F_2. The concerned free-energy component may the expressed as [4] $\frac{k_B T}{2}\sum_{i,j} c_j(\mathbf{r}) c_j(\mathbf{r}') \Omega_{ij}(\mathbf{r} - \mathbf{r}') d^3\mathbf{r} d^3\mathbf{r}'$ where Ω_{ij} is the weighted potential, defined as $\Omega_{ij} = 1 - \exp(-\omega_{i,j}(|\mathbf{r} - \mathbf{r}'|)/k_B T$. Here c_j is the concentration of the jth ionic species, and $\omega_{i,j}$ is the nominal short-range hydration interaction between ions of species i and j. For calculations, $\omega_{i,j}$ can be treated using a virial expansion of the grand canonical potential, retaining up to quadratic terms [4], or alternatively from a field-theory expansion of the grand partition function [4].

A dynamic coupling between the order-parameter variation (representing the hydrophobic interactions) and the EDL potential distribution can now be explicitly established by first noting that for electrochemical equilibrium, $\delta F_2/\delta\psi = 0$, and $\delta F_2/\delta c_i = 0$, where ψ is the EDL potential distribution. These constraints can be invoked in consistency with the Poisson equation [1], independent of the Boltzmann distribution that ceases to be valid under overlapped EDL conditions. Additional non-PB interactions, originating as a consequence of the rapid fluctuations in the density profiles close to the interface (disregarding the concerned charges) on account of hydrophobic interactions, can be captured by introducing the following correction term [5]: $\psi_{\text{add}} = -k_B T \ln[\rho(z)/\rho_l]$, where $\rho(z)$ is the density profile in the solvent and ρ_l is the density of the bulk liquid. Setting the order parameter ϕ in such a manner that $\phi = -1$ represents the liquid, whereas $\phi = 1$ represents the vapor phase, $\rho(z)$ can be expressed in terms of the order-parameter profile as $\rho = \rho_l - 0.5(\rho_l - \rho_v)(1 + \phi)$, where ρ_v is the density of the vapor phase. The variations in ϕ, necessary for estimating the density profiles, are obtained from the free-energy description, consistent with the surface-wettability condition that explicitly relates the contact angle (θ_w) with the surface value of the order parameter (ϕ_s) as [3] $\cos\theta_w = \frac{3\phi_s - \phi_s^3}{2}$. With these considerations, an explicit interlinkage is established between the hydrodynamic and electrical description through the order-parameter variation.

In order to assess the predictive capability of the present model vis-à-vis benchmark MD simulations [6], fluidic transport through rectangular-shaped nanochannels is considered, in the presence of EDL effects. To render the present simulation studies comparable with benchmark literature, the following simulation parameters are considered [6]: $\gamma_{lv} = 0.07$ N/m, $\frac{k_B T}{\varepsilon_1} = 1$ (where ε_1 is the depth of the Lennard-Jones potential well), $\rho_l \sigma^3 = 1$ (where σ is the collision parameter), and $\sigma = l_B = e^2/4\pi\varepsilon k_B T = 0.7$ nm (where ε is the permittivity of the medium). Other phase-field parameters are taken from reported literature [3]. The solvent considered here contains monovalent counterions to which monovalent salt ions are added (size of micro-ions = size of solvent ions). Gap between the upper and lower confining walls (H) is kept as 20.8σ. Charge per unit surface on these walls is taken as $Q = -0.2e\sigma^2$, while the Gouy-Chapman length is taken as $1/\kappa = (2\pi l_B Q)^{-1} = 0.8\sigma$. The Poisson equation with potential corrections is employed, in conjunction with the Cahn-Hillard Navier-Stokes equations [4], to obtain the potential and velocity distributions. Periodic boundary conditions are applied along the axial and lateral directions over a period of 16σ. The micro-ion concentration ($\rho\sigma^3$) is varied between 15×10^{-3} to 0.16, which corresponds to a bulk ionic strength ranging from 10^{-2} M to 1 M. Surface values of the order parameter are set by considering the following two separate cases: (a) wetting case: $\theta_w = 80°$, and (b) nonwetting case: $\theta_w = 140°$.

Figure 1 depicts the micro-ion density profiles (averaged over the lateral directions), as against the corresponding from MD simulation predictions [6]. These results clearly demonstrate that the present mesoscopic model successfully captures the structuration effects close to the confining charged walls, through the manifestation of a typical damped oscillatory nature of the micro-ionic density profiles. For analyzing the flow field within the EDL, a pure pressure-driven flow is first considered (corresponding to an average driving force of $0.02\varepsilon/\sigma$). Traditionally, the apparent ζ potential is defined as a linear response of the streaming current (advective transport of micro-ions), I_s, as follows [1]: $I_s = -\varepsilon\zeta A F_{\mathrm{av}}/\eta$ where F_{av} is the average externally applied volumetric force that is equivalent to the imposed pressure gradient, ε is the permittivity of the medium, A is the cross-sectional area of the conduit, and η is the fluid viscosity. While this classical definition appears to demand further generalization (as we see later), we start with the same as a basis for describing the hydrodynamics within the EDL on wetting and nonwetting substrates. For the wetting case, the location of the plane of zero slip virtually coincides the edge of the "Stern layer" (layer thickness $\sim z_s = \sigma$), as seen from Fig. 2. Since this layer contains only immobile ions, the net effect is a reduction of the advection (streaming) current. However, for the nonwetting case, hydrophobic interactions give rise to an apparent wall slip, characterized by a slip length, b (defined as $u_w = b\frac{\partial u_l}{\partial z}|_w$, by extrapolating the tangent to the liquid-phase velocity profile up to the adjacent wall).

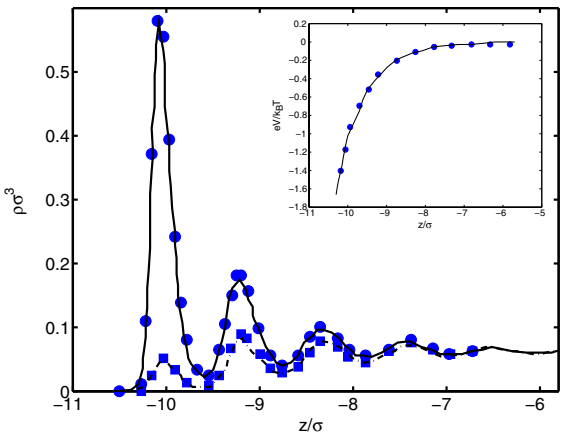

FIG. 1 (color online). Micro-ionic density profiles (averaged over the lateral dimensions), as a function of the normalized separation distance, for the wetting case. The solid and dashed lines represent counterion and co-ion density predictions, respectively, from the present model, whereas the circular and rectangular markers represent the corresponding MD predictions [6]. The corresponding predictions of electrostatic potential are shown in the inset. The oscillations in the ionic density profiles are clear manifestations of the confinement-induced structuration effects, as induced by the discreteness of the solvent molecules. The potential corrections in the mesoscopic description enable one to capture the underlying consequences, without necessarily executing molecular simulations.

This case is represented in the inset of Fig. 2. The corresponding velocity and charge density profiles, as well as slip length prediction ($b \approx 11\sigma$), match well with the corresponding MD simulation predictions.

Substantiated by the quantitative capabilities of the present mesoscopic model in reproducing the upscaled MD simulation predictions illustrated as above, we next summarize our new important findings with regard to the explicit dependence of the nondimensional zeta potential as a function of a nondimensional slip length, for a general class of combined pressure-driven and electro-osmotic flows. For such a case, we decompose the net axial field (E_{net}) into two components: one corresponding to an applied field (E_{app}) and the other corresponding to an induced field due to ion advection, or the so-called "streaming" field (E_s). The net current is a sum of the advection current [$I_{\mathrm{adv}} = \int_A e(c_+ - c_-)udA$] and the diffusion current [$I_{\mathrm{diff}} = \frac{e^2(E_{\mathrm{app}}+E_s)}{f}\int_A(c_+ + c_-)dA$]. The ionic concentration distributions, in turn, can be obtained from the modified PB distribution with potential correction, as $c_\pm = c_0 \exp(\mp e\frac{\psi-\psi_{\mathrm{add}}}{k_B T})$ where c_0 is the bulk ionic concentration. A generalized definition of the streaming current follows from the steady-state electroneutrality constraint for a pure pressure-driven flow, i.e., $I_{\mathrm{adv}} + I_{\mathrm{diff}} = 0$ when $E_{\mathrm{app}} = 0$, so that $I_{\mathrm{adv}} \equiv I_s$ for that case. By following this definition, the velocity profile for a general case can be

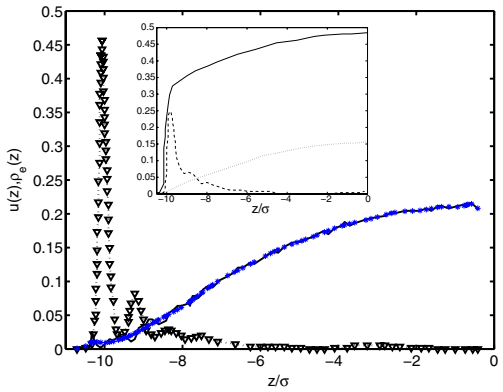

FIG. 2 (color online). Pressure-driven velocity profile (solid line represents MD predictions [6], whereas the "starred" line represents predictions from the present model) and charge density profile (dotted line with triangular markers) in normalized units, for the wetting case. The physical situation is equivalent to the location of a "no-slip" plane at a distance σ from the wall. Within this wall-adjacent layer, the system is virtually immobile. The nonwetting case is presented in the inset. The solid and dashed lines represent velocity and charge density profiles, whereas the dotted line represents hydrodynamic prediction with a no-slip boundary condition. A portion of the velocity profile with steep local gradients adjacent to the wall represents the velocity variation within a two-phase layer, the inception of which is triggered by hydrophobic interactions. The effective slip length is obtained as an extrapolation of the velocity profile prevailing over the remaining extent of the solvent phase. Agreement with MD predictions [6] is excellent.

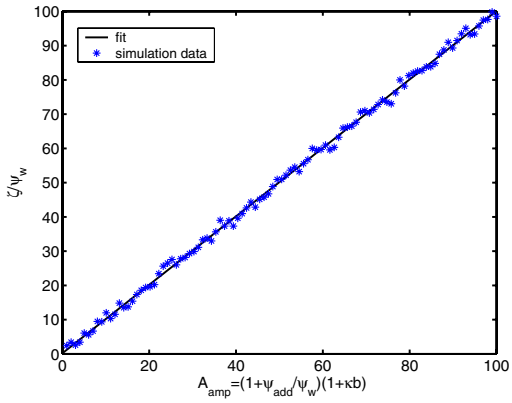

FIG. 3 (color online). Effective ζ potential as a function of the amplification factor A, for the nonwetting case. The reported results appear to exhibit a universal trend, irrespective of the details of the flow actuation mechanism (pressure-driven, electro-osmotic, or a combination). For simulating combined effects, axial electric fields of varying strengths are considered, both in the sense of aiding and opposing the imposed pressure gradient. For large ψ_w, replacement of κ with $\frac{\partial(\psi/\psi_w)}{\partial z}|_w$ identical fits.

expressed explicitly in terms of the applied pressure gradient as well as the imposed electrical field (noting that E_s can be expressed explicitly as a function of the imposed pressure gradient, in turn, by referring to the electroneutrality constraint of a pure pressure-driven flow at steady state). The relationship between the driving field and the ζ potential, thus, is nonlinear in general, for combined pressure-driven and electro-osmotic flows. Despite this complexity, we look for a synergy in the effective ζ potential-slip flow dependence, by plotting the variations in $\frac{\zeta}{\psi_w}$ as a function of $A_{\text{amp}} = (1 + \frac{\psi_{\text{add}}}{\psi_w})(1 + \kappa b)$ for the nonwetting case, as depicted in Fig. 3. Since the nonwetting case is not characterized with the presence of a zero-slip plane within the domain of electrochemical transport, the traditional linear relationship between the advection current and the average driving force is employed for that case in deriving an equivalent ζ potential. Remarkably, all the simulation data in Fig. 3 cluster around the variation $\frac{\zeta}{\psi_w} = A_{\text{amp}}$, within an error bound of $\pm 1\%$. This reveals that the augmentation of electrokinetic effects through an enhanced ζ potential on account of apparent slip due to hydrophobic interactions follows a somewhat universal trend, independent of the driving flow actuation mechanisms (pure pressure-driven, electro-osmotic, or their suitable combinations), so long as the equivalent ζ potential is evaluated from the following extended classical definition of the advection current: $I_{\text{adv}} = -\frac{\varepsilon \zeta A F_{\text{ext,av}}}{\eta}$. It is important to mention here that $F_{\text{ext,av}}$ are, respectively, taken here as the net average external volumetric driving force and the net rate of advective transport of charges under a combined consequence of all driving influences, and not necessarily on the basis of the streaming current definition corresponding to a pure pressure-driven flow. The universal nature depicted in Fig. 3 is physically reminiscent of the fact that the hydrodynamics within the EDL in narrow fluidic confinements is a sole function of the intrinsic interactions between the electrolyte-substrate combination, and by no means on the exact driving mechanisms that pump the bulk fluidic transport. Importantly, hydrophobic interactions in this generalization feature not only in the description of the apparent slip length (b), but also in the definition of ψ_{add}. One remarkable physical consequence of this conjecture is that apparent slip due to hydrophobic interactions results in an amplification of the ζ potential by an amplification factor A_{amp}. Large values of A_{amp}, indeed, may be realized by designing superhydrophobic nanochannel substrates, as a consequence of large values of ψ_{add} and b.

The above effective amplification in the interfacial slip may be realized in practice by designing patterned undulations on nonwetting substrates of nanofluidic channels, so as to simultaneously trigger a generic and spontaneous phase transition and an augmentation in the effective EDL potential. On one hand, the low density vapor phase is likely to amplify the level of slippage by physically acting as a ''low-friction blanket'' that effectively prevents the liquid from being directly exposed to the surface irregularities. This, on the other hand, amplifies the effective surface potential and augments the rate of net ionic transport, in a manner that is independent of the details of the bulk driving influences. Based on this conjecture, one may innovate new experiments or devices towards exploring the practical realizability of ''supertransportive'' nanofluidic systems by exploiting the strongly coupled electromechanics and hydrodynamics within the EDL.

*suman@mech.iitkgp.ernet.in

[1] R. J. Hunter, *Zeta Potential in Colloid Science* (Academic, New York, 1981); F. H. J. van der Heyden, D. Stein, and C. Dekker, Phys. Rev. Lett. **95**, 116104 (2005); S. Chakraborty and A. K. Srivastava, Langmuir **23**, 12421 (2007); D. Paul and S. Chakraborty, J. Appl. Phys. **102**, 074921 (2007); S. Chakraborty, Anal. Chim. Acta **605**, 175 (2007); S. Das and S. Chakraborty, AIChE J. **53**, 1086 (2007); S. Das, K. Subramanian, and S. Chakraborty, Colloids Surf. B **58**, 203 (2007); S. Chakraborty, J. Phys. D **39**, 5356 (2006); S. Chakraborty and D. Paul, J. Phys. D **39**, 5364 (2006); S. Das and S. Chakraborty, J. Appl. Phys. **100**, 014098 (2006); S. Das and S. Chakraborty, Anal. Chim. Acta **559**, 15 (2006); S. Das, T. Das, and S. Chakraborty, Sens. Actuators B Chem. **114**, 957 (2006); S. Das, T. Das, and S. Chakraborty, Microfluid. Nanofluid. **2**, 37 (2006).
[2] S. Granick *et al.*, Nat. Mater. **2**, 221 (2003); S. Chakraborty, Appl. Phys. Lett. **90**, 034108 (2007).
[3] S. Chakraborty, Phys. Rev. Lett. **99**, 094504 (2007).
[4] Y. Burak and D. Andelman, J. Chem. Phys. **114**, 3271 (2001).
[5] S. Marcelja, Langmuir **16**, 6081 (2000).
[6] L. Joly, C. Ybert, E. Trizac, and L. Bocquet, Phys. Rev. Lett. **93**, 257805 (2004).